Science of the Total Environment 695 (2019) 133746

Contents lists available at ScienceDirect

Science of the Total Environment

journal homepage: www.elsevier.com/locate/scitotenv

Radon mitigation by soil depressurisation case study: Radon concentration and pressure field extension monitoring in a pilot house in Spain

Marta Fuente [a,b,c], Daniel Rábago [d], Jamie Goggins [b,c], Ismael Fuente [d], Carlos Sainz [d], Mark Foley [a,*]

[a] School of Physics, National University of Ireland Galway, Ireland
[b] Civil Engineering, School of Engineering, National University of Ireland Galway, Ireland
[c] MaREI Centre for Marine, Climate and Energy, Ryan Institute, National University of Ireland Galway, Ireland
[d] Radon Group, University of Cantabria, Spain

HIGHLIGHTS

- Active and passive soil depressurisation (SD) ability was studied in a pilot house.
- Radon concentration and pressure field extension (PFE) under slab were monitored.
- Radon behaviour was analysed under the influence of atmospheric parameters.
- Pressure drop with distance was found proportional to depressurisation under slab.
- Over 85% radon reduction was achieved for active and passive SD.

GRAPHICAL ABSTRACT

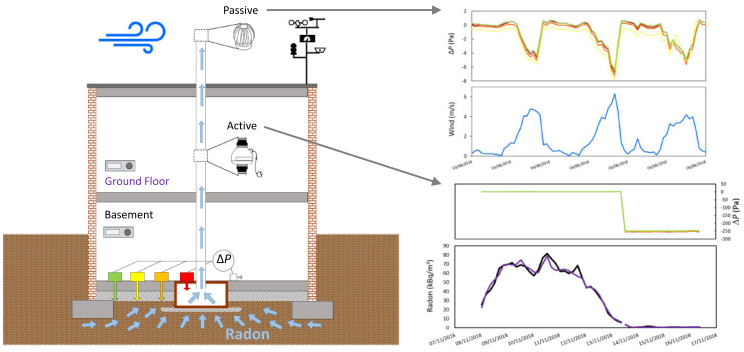

ARTICLE INFO

Article history:
Received 20 May 2019
Received in revised form 14 July 2019
Accepted 1 August 2019
Available online 05 August 2019

Editor: Pavlos Kassomenos

Keywords:
Radon mitigation
Soil depressurisation
Pressure field extension
Permeability

ABSTRACT

A one-year monitoring study was conducted in a pilot house with extremely high radon levels to investigate the ability and efficiency of radon mitigation by soil depressurisation (SD) both active and passive. The study included monitoring of radon concentration, pressure field extension (PFE) under the slab and some atmospheric parameters for different testing phases. Periods in which the house remained closed to foster radon accumulation were alternated with phases of active and passive soil depressurisation under different conditions. The behaviour of the radon concentration in the pilot house was analysed along with the influence of atmospheric variables, significant correlations were found for the radon concentration with atmospheric pressure, outdoor temperature and wind. From the PFE analysis it was proven that the pressure drop with distance from the suction point of the SD system is proportional to the depressurisation generated. A behaviour law was found for the permeability characterisation of the house based on the active SD performance and also, the relationship between wind velocity and extraction airflow during passive SD operation by means of a rotating cowl was obtained. Radon reductions in excess of 85% were achieved for the different testing phases in all cases. Finally, from the results it was

* Corresponding author.
E-mail addresses: m.fuentelastra1@nuigalway.ie (M. Fuente), mark.foley@nuigalway.ie (M. Foley).

https://doi.org/10.1016/j.scitotenv.2019.133746

postulated that a fan power of 20 W is sufficient to ensure radon reductions over 85% for dwellings with similar aggregate layer and soil permeability.

1. Introduction

Radon (^{222}Rn) is a colourless, odourless, radioactive gas formed in the ground by the radioactive decay of uranium (^{238}U), which is present in all rocks and soils of the Earth's crust. With a half-life of 3.8 days together with its noble gas condition, radon can move through interconnected pores in the soil, reach the Earth's surface and penetrate into buildings. Radon is the greatest natural source of exposure to ionising radiation for the general public and it is also the leading cause of lung cancer after smoking, as stated by the World Health Organisation (WHO, 2009). Poor ventilation conditions, gaps or cracks in the construction systems favour the accumulation of radon inside buildings, leading to health risks related to the inhalation of the radon decay products. 9% of deaths from lung cancer per year are attributable to residential radon exposure in the European Union, which accounts for more than 20,000 deaths each year (Darby et al., 2004; WHO, 2018).

There are various prevention and mitigation measures that might be considered to minimise indoor radon concentration, in order to address the radon problem both in new and existing buildings. Radon protection strategies include reduction of radon entry by sealing of surfaces, barriers or membranes, soil depressurisation (SD) techniques to reverse the air pressure differences between the indoor occupied space and the soil underneath the building, and ventilation of spaces to dilute indoor radon concentration with external air (Long et al., 2013; Jiranek, 2014; WHO, 2018).

The active and passive SD techniques have proven to be the most effective strategy for indoor radon prevention and mitigation. SD systems include three basic components: a suction point, ideally located in a continuous and uniform permeable aggregate layer under the slab, an exhaust pipe to extract the soil gas and a means of extraction, which can be a mechanical fan in the case of forced extraction or a chimney or cowl for passive depressurisation using natural extraction and wind effect. The suction point is normally a sump placed under the slab or on a side of the building, connected to a permeable aggregate layer, but perforated pipes beneath the existing floors can be an alternative to sumps. The building characteristics (airtightness of the building, exhaust pipe diameter and height, type of extractor, etc.) have an impact in the SD performance; likewise, it can be affected by the stack effect due to temperature difference, meteorological conditions, ventilation systems and occupancy behaviour (DELG, 2002; Abdelouhab et al., 2010; Long et al., 2013; Diallo et al., 2015).

Previous works discuss the importance of the aggregate layer in the design of SD systems for radon mitigation. The impact of the granular fill materials permeability of such aggregate layer and the soil permeability beneath and surrounding the building on the SD effectiveness has been investigated and permeability characterisation of aggregates within the European context conducted (Hung et al., 2018a, b; Fuente et al., 2019). But there is a lack of evidence in testing efficiency of SD techniques in relation with the pressure distribution in actual buildings with elevated radon concentration where radon reduction can be quantified with confidence.

This paper outlines a case study on radon mitigation by soil depressurisation in an unoccupied real building built for experimental purposes. A one-year monitoring study was conducted in a pilot house with very high radon levels to investigate the ability and efficiency of active and passive SD. The work includes the behaviour analysis of the radon concentration inside the experimental building. Also, it presents the analysis of the SD effectiveness, looking at the pressure distribution induced under the building slab, in relation to the permeability characterisation of the aggregate layer beneath the slab, and the achievable radon reduction in such conditions.

2. Materials and methods

2.1. Pilot house: location and design

The pilot house chosen for the case study is located in Saelices el Chico, Salamanca (Spain) within the land of a former uranium mine managed by the company ENUSA Industrias Avanzadas S.A. (see Fig. 1) now under reclamation activities. The location of the experimental house was selected due to the high radon exhalation rate and the high radium content in the soil of the area, which would provide high radon levels accumulated inside the building. An average radium concentration of 1600 Bq/kg was quantified from different soil samples taken onsite, this value is 40 times in excess of the average worldwide concentration, approximately 40 Bq/kg (Frutos et al., 2011). The experimental house was built in an area where there was no mining activity. In terms of the geology characteristics, the site belongs to the Iberian Massif and the predominant host rocks are schist and quartzite (IGME, 2015).

The experimental house was designed to reproduce a space large enough to be representative of a room in a typical dwelling house. It consists of two storeys, a partially below grade so-called basement of 2 m height and a ground floor (2.41 m height) connected by a standard door. The dimensions of the rooms are 5×5 m^2 (see Fig. 2). There are two windows at the ground floor level, one in the front wall next to the main door and another one in the opposite wall. The front wall of the house is facing the North.

In 2006 when the pilot house was built for a different study, several mitigation measures were investigated (Frutos, 2009). As a result, there are two soil depressurisation systems installed in the house. Both SD systems consist of a 1 m^2 and 0.5 m deep sump and an exhausting pipe of 125 mm diameter, one system is located in the centre of the experimental house with the sump placed in the aggregate layer below the concrete slab and the other system is placed on a side of the house (see Fig. 2).

Materials used for the construction of the house were according the Spanish building practices, a 15 cm thick aggregate layer was placed below a 10 cm thick concrete slab. Standard clay bricks were used for the walls and conventional perforated clay bricks to build the sumps of the SD systems (Frutos et al., 2011).

2.2. Monitoring system

To continuously monitor radon concentration several active radon monitors were used, including the Radon Scout (SARAD GmbH), Radon Scout Home (SARAD GmbH) and AlphaE (Bertin Instruments) detectors. Performance of the radon monitors used in the experiment at the pilot house was tested previously in a purpose-built radon chamber (Fuente et al., 2018). Radon concentration was recorded in the basement and in the ground floor.

For some measurement periods, the radon monitors used were contaminated due to the high radon exposure levels at the pilot house. These monitors were then replaced. There were also some problems due to memory of the devices in some cases, so there is radon data missing for some of the testing phases.

A pressure sensor system was installed to monitor the distribution of pressure under the slab of the house. The pressure system was

Fig. 1. Map of Spain and plan of the mining facilities indicating the location of the pilot house and a recent picture of the building.

specifically developed for this experiment at the pilot house in collaboration with a research group of the ITEFI-CSIC, Madrid (Spain). It is an acquisition system designed with segmented architecture and capacity up to 15 pressure sensors. It consists of an adaptor board for the pressure sensor units and contains a series of Honeywell pressure sensors (HSCDRRD006MDSA3 model, operating pressure $\pm$ 6 mbar, accuracy 0.25%) with SPI communication. The connections between the units use Ethernet cables connected in parallel and the adaptor board needs to be connected to a PC by an input/output USB card type Lab Jack U3. The actual system installed in the house for this experiment consists of a total of 8 pressure sensor units. There are 5 of them distributed along the basement area in different holes drilled through the concrete slab to measure pressure difference in the aggregate layer under the slab and the inhabited volume of the basement, at distances $d = 1, 2$

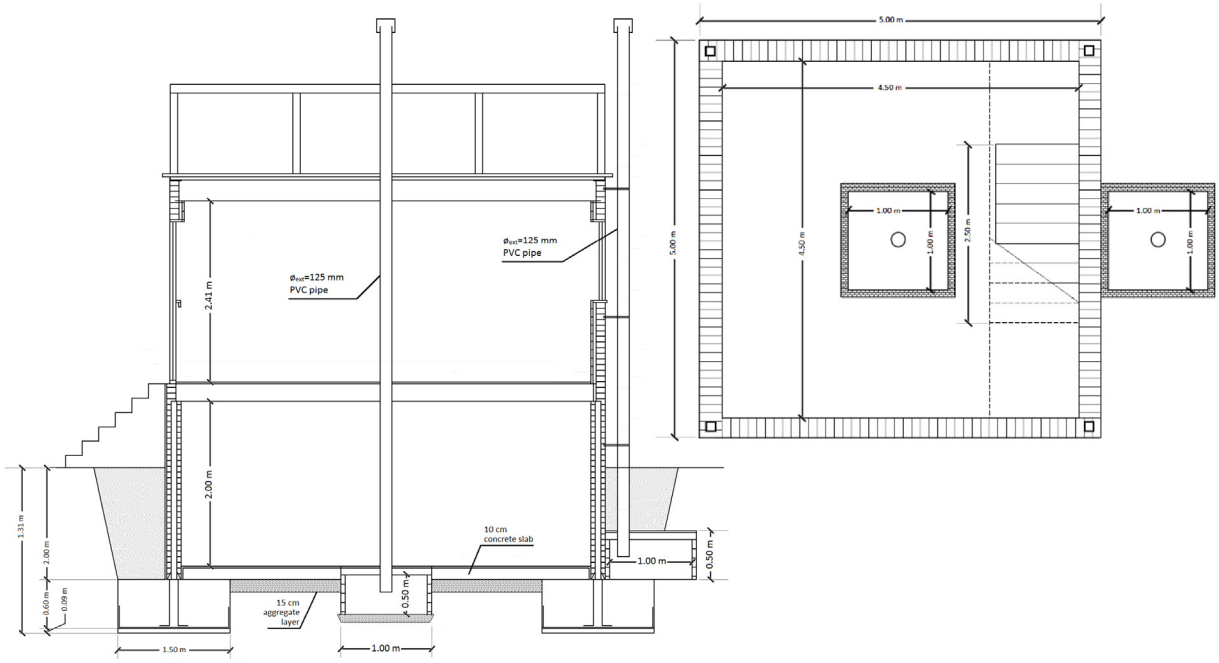

Fig. 2. Section view of the house and plan of the basement after installation of mitigation measures, modified from Frutos et al. (2011).

and 2.4 m from the central sump. The remaining 3 pressure sensors are placed at the sump and pipe of the central SD system and at room level for reference.

To record atmospheric conditions locally at the house site, a local weather station (PCE-FWS20, PCE Instruments) was installed on the rooftop. Variables recorded were wind velocity, indoor and outdoor temperature, atmospheric pressure, relative humidity and accumulated rain. Both the pressure sensor system and the weather station are remotely accessible, which facilitates data collection.

2.3. Experimental methodology

The initial monitoring plan was alternating testing phases of SD performance (active or passive) with periods in which the house remained completely closed, in order to record radon increase and reduction over the different phases along with the pressure field extension induced under the slab, hereinafter referred as PFE.

The monitoring study commenced in June 2018 with a first phase of the house closed to foster accumulation of radon gas. All testing phases with this setting, in which the house remains closed and the pipes of the SD systems capped to foster radon accumulation in the building, will be henceforth referred as closed periods. During the closed periods, there is no ventilation mechanism apart from the natural ventilation due to air leakage of the house and there is no heating mechanism used. After the first closed period (phase 1), a phase 2 involved passive SD performance evaluation. Then a subsequent series of closed periods followed by active SD performance was conducted up to 9 phases, with different active SD settings, ending in April 2019.

Only the central SD system was used for the investigation of the soil depressurisation during the SD testing phases. A rotating cowl was used for the passive SD operation and for the active SD performance, a mechanical fan (RP145i, RadonAway with 80 W max) was installed in the central SD system pipe. The mechanical fan was modified by adding a potentiometer to control the extraction airflow, which in terms of velocity ranges from 0 to 4 m/s. A hot wire anemometer (Testo 440, measuring range 0 to 30 m/s, accuracy $\pm$(0.3 m/s + 4% of mv) and resolution 0.01 m/s) was used to measure extraction velocity of the mechanical fan punctually, to obtain the relationship between the extraction airflow and the mechanical fan power. A schema of the experimental house settings for the different phases is shown in Fig. 3.

The duration of the different phases varied, depending on the access to the site and technical problems experienced with the sensors or the power supply. The monitoring study was stopped at some times and later resumed.

From February 2019, a stage of the monitoring study focused on the investigation of the mechanical fan extraction impact on the SD

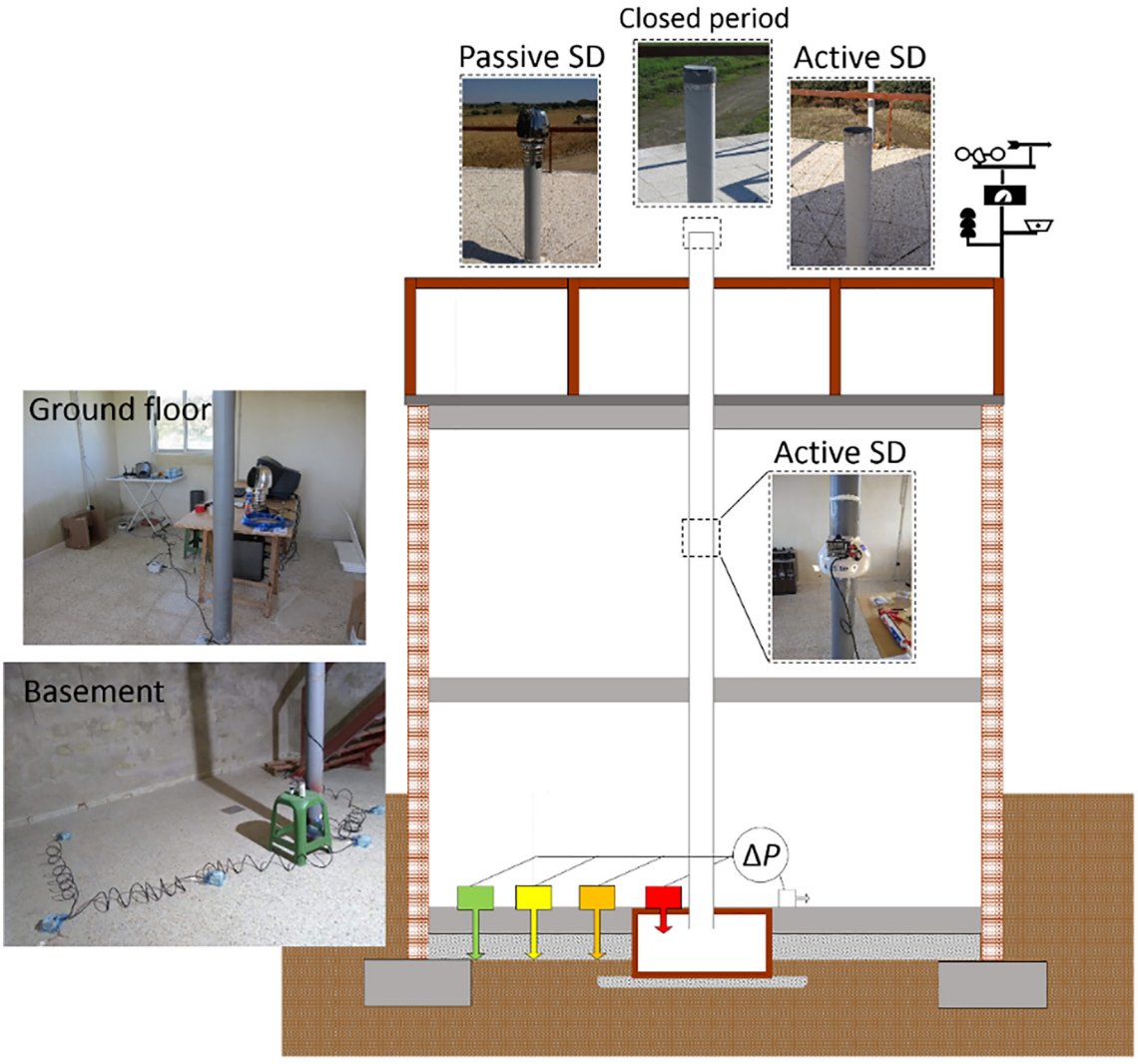

Fig. 3. Schema of the pilot house for the closed periods, active SD and passive SD testing phases. Section view of the experimental house shows the pressure sensors system in the basement (same for all phases), the mechanical fan installed on the central pipe (for the active SD performance) and the top of the exhaust pipe in the house rooftop, with a cap, a rotating cowl or opened, depending on the testing phase.

Table 1
Summary of testing phases at the pilot house.

Phase	Description	Dates
1	Closed period	25/06/2018–26/07/2018
2	Passive SD	26/07/2018–end of August
No measurements (issues related with the pressure sensors)		
3	Closed period	10/10/2018–13/11/2018
4	Active SD (v_{ext} = 0–4 m/s)	13/11/2018–16/11/2018
No measurements (issues related to power supply in the house)		
5	Closed period	13/12/2018–19/02/2019
6	Active SD (v_{ext} = 1.5 m/s)	19/02/2019–06/03/2019
7	Closed period	06/03/2019–14/03/2019
8	Active SD (v_{ext} = 2 m/s)	14/03/2019–02/04/2019
9	Closed period	02/04/2019–30/04/2019

effectiveness was conducted. It consisted of short periods (1–2 weeks) of active SD followed by closed periods, gradually increasing the mechanical fan extraction for the SD performance by controlling the airflow rate.

A summary of the testing phases including dates and incidents are presented in Table 1.

Radon levels were monitored continuously, but also, passive radon detectors were used for some testing periods. However, due to the high radon concentration, the passive track etched detectors were saturated in the most cases.

3. Radon concentration behaviour in the pilot house

There is a long term record of the radon concentration fluctuations in the experimental house measured during the different testing phases. Before looking at the radon reductions generated as a result of the soil depressurisation, it is important to try to understand the natural behaviour of the radon concentration inside the house. To do so, the closed testing periods when there were no mitigation measures in operation and the house remained closed with the exhaust pipes of the SD systems capped are analysed.

Indoor radon levels in the experimental house depend on three features: the radon source, the entry rate and the air exchange between the building and the outdoor air, all of which, in turn, depend on many other variables and especially atmospheric conditions.

The radon source is constituted by the soil beneath and surrounding the house, which contains high radium levels. Therefore, it is expected to find higher radon levels in the basement, which is partially below grade and in direct contact with the soil, than in the ground floor. An overview of the radon levels recorded is presented in Fig. 4.

An average radon concentration of 55 kBq/m^3 is found in the basement for the closed house conditions, while for the ground floor there is an average radon concentration of 26 kBq/m^3 under the same house settings. Both values are obtained from the radon records available during the closed testing periods. The average radon concentration values from the initial study conducted in 2006 are 40 kBq/m^3 for the basement and 7 kBq/m^3 for the ground floor. These values were obtained from a three month measurement period (January–April) in which the experimental house remained closed building up the radon concentration, before the installation of any mitigation measures (Frutos et al., 2011). The difference may be related to the deterioration of the basement slab associated with thermal dilation or other analogous phenomenon, therefore leading to the formation of new cracks or radon pathways. The higher increase of the ground floor radon concentration compared to the basement's with regard to the initial levels by Frutos et al. (2011) could also be due to the fact that the door between floors was not closed during all the testing phases as it was for the initial study.

The concentration ratio between floors found for the closed house testing configuration is approximately two, which means that the concentration recorded in the basement is approximately double the concentration in the ground floor. This result is according to expectation, as the basement is in direct contact with the soil and the main radon gas entry is through gaps or cracks in the foundation, while the radon in the ground floor comes from the radon in the basement. The infiltration through the main door and the windows could be considered as a source of radon gas, but the outdoor air radon concentration at the site is much lower, approximately 300 Bq/m^3. Then, assuming that radon in the ground floor comes only from the basement, the lower radon concentration in the ground floor is explained by the radioactive decay and the exchange of outdoor air through infiltration.

3.1. Radon behaviour and atmospheric parameters

Fluctuations of radon concentration are daily and seasonal, and they are related to atmospheric conditions and the air exchange between the building and the outdoor air. There is also a seasonal component related to the outdoor temperature changes and the associated atmospheric pressure variations that directly affects radon entry in the building (Nero et al., 1990; Scivyer and Jaggs, 1998).

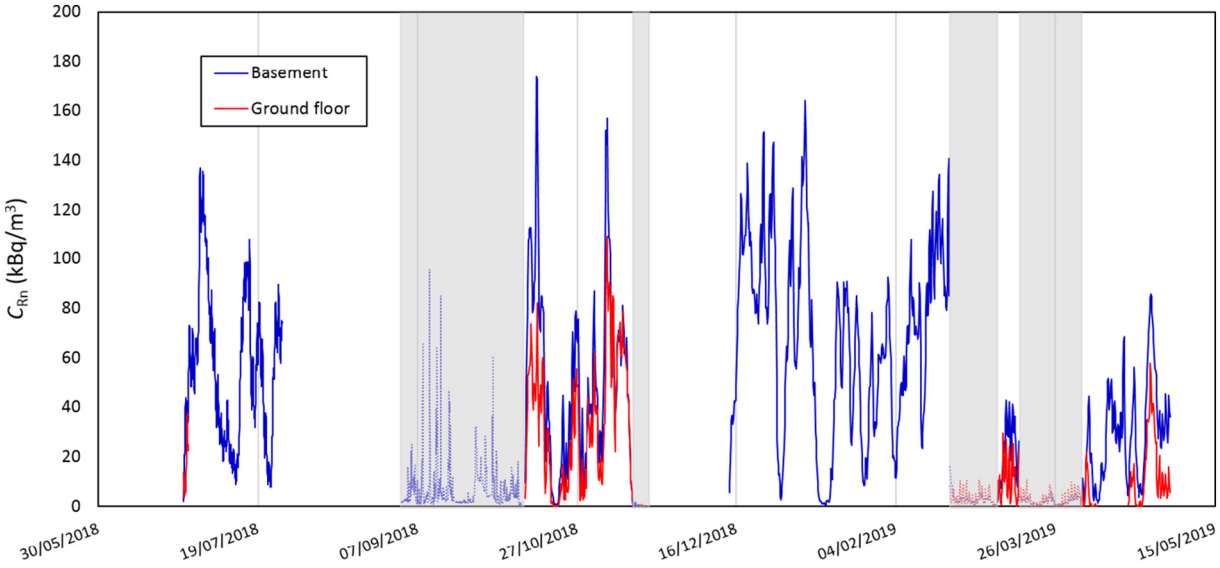

Fig. 4. Radon concentration recorded in the basement and ground floor of the pilot house. The solid line indicates the closed testing periods and the dashed line (shaded areas) indicates the periods of SD performance.

The air exchange rate in the experimental house reaches its minimum value during the closed testing periods as there is no ventilation mechanism, apart from the air leakage through the windows and main door frames. Thus, the radon levels in the house basically depend on the atmospheric conditions, which determine the soil gas pressure-driven flow from the ground into the building.

Multiple atmospheric conditions influence radon concentrations and it is possible to find correlations between the trends in radon concentration and atmospheric variables (Schubert et al., 2018; Garcia-Tobar, 2019). The radon concentration trends as a function of the different atmospheric parameters recorded were analysed for the closed testing periods in the pilot house. Selected measurement periods where statistically significant correlation was found between the radon concentration in the pilot house and a specific atmospheric variable are presented below.

The differences between indoor and outdoor temperature in a building can generate a pressure gradient due to the stack effect, leading to an increase of the soil gas flow from the ground into the basement through the existing entry routes. Pressure gradient due to stack effect is described as follows:

$$\Delta P = c\, P_{\text{atm}} h \left(\frac{1}{T_{\text{out}}} - \frac{1}{T_{\text{in}}} \right) \quad (1)$$

where ΔP is the indoor-outdoor pressure difference, $c = 0.0342$ K/m is a constant, P_{atm} is the atmospheric pressure in Pa, h is the height or distance in m, T_{out} and T_{in} correspond to outdoor and indoor temperature respectively (Frutos, 2009).

Fig. 5 depicts an example of the pressure difference generated as a result of the stack effect in the pilot house along with the radon concentration recorded for a time period when the house was closed. Pressure difference was calculated from the indoor and outdoor temperature records (see Fig. 5) following Eq. (1), using the height of the house $h = 4.7$ m and assuming a constant atmospheric pressure $P_{\text{atm}} = 10^5$ Pa.

From Fig. 5, positive correlation between outdoor temperature and radon concentration is found at a daily scale, agreeing with previous studies (Mentes and Eper-Papao, 2015; Schubert et al., 2018). A Pearson's correlation coefficient of $r = 0.44$ with a 95% confidence level is obtained.

Looking at the pressure difference ΔP result of the stack effect, fluctuations are within the range of −1 to 3 Pa. A Pearson's correlation coefficient of $r = -0.48$ is obtained between radon concentration in the ground floor and the pressure difference ΔP generated due to the indoor temperature at the ground floor and outdoor temperature difference. As the pressure difference increases, radon concentration decreases. The negative pressure difference ΔP means that indoor pressure in the house is lower than the pressure in the soil and thus, the radon in the soil flows into the house, while when ΔP is positive the pressure inside the house is higher and the entry of soil gas is reduced.

The wind effect can generate a pressure gradient too, due to the pressure changes and suction generated in the walls, which can modify the indoor pressure relative to that in the ground. But also, the wind causes the opposite effect as it fosters ventilation through infiltration that lower the radon levels (Burke et al., 2010; Baskaran, 2016). A negative correlation between the radon concentration and the wind was found, as wind velocity increases the radon level decreases as observed in Fig. 6(a). For this case an $r = -0.59$ Pearson's correlation coefficient is obtained with 95% confidence level. This result is also consistent with the literature (Riley et al., 1996; Schubert et al., 2018).

Theoretically, pressure variation inside a dwelling is almost simultaneous with atmospheric pressure changes, but pressure changes in the soil pores beneath the building reach the atmospheric pressure values with a time delay that depends on the soil characteristics (e.g. porosity). Thus, there is a pressure gradient generated between the soil and inside the building that determines the soil gas airflow into the building (Frutos, 2009). If the atmospheric pressure decreases and so it does indoor pressure of the house, indoor pressure in the house is lower than the pressure in the soil beneath, which leads to an increase of the radon flow into the house. From the analysis of the experimental data

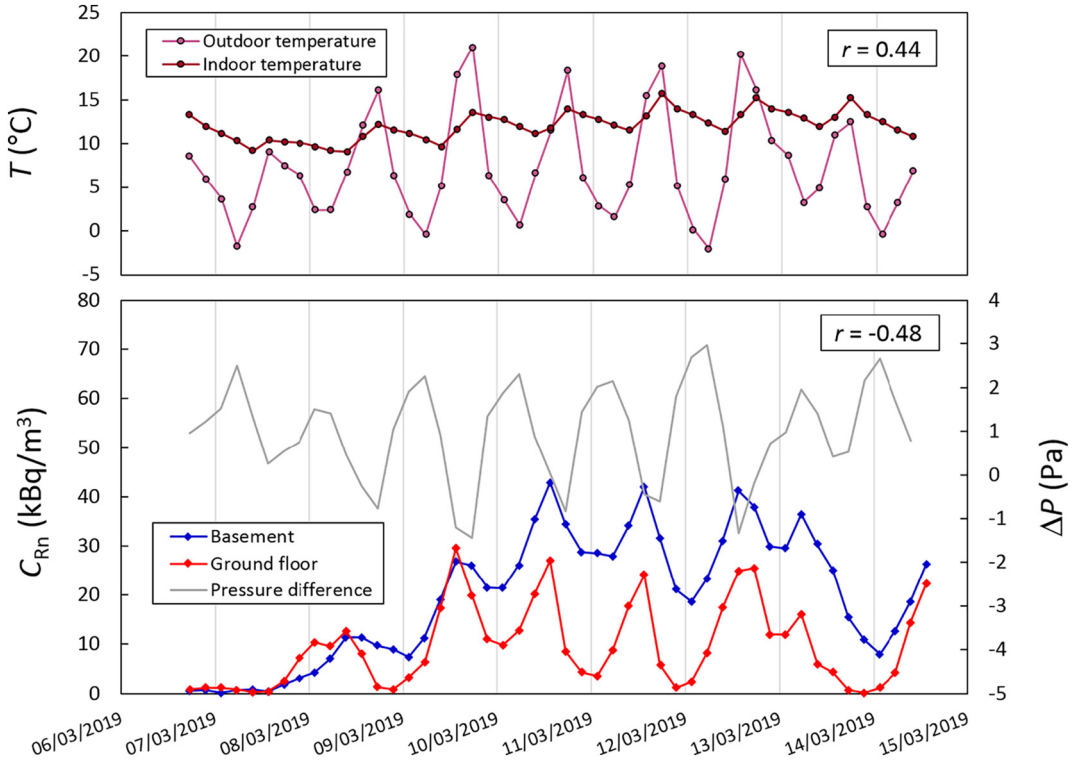

Fig. 5. Radon concentration recorded in the basement and ground floor of the pilot house along with the pressure difference ΔP obtained as a result of the indoor – outdoor temperature for a time period while the house was closed. Pearson's correlation coefficient r between the radon concentration, pressure difference and outdoor temperature are indicated.

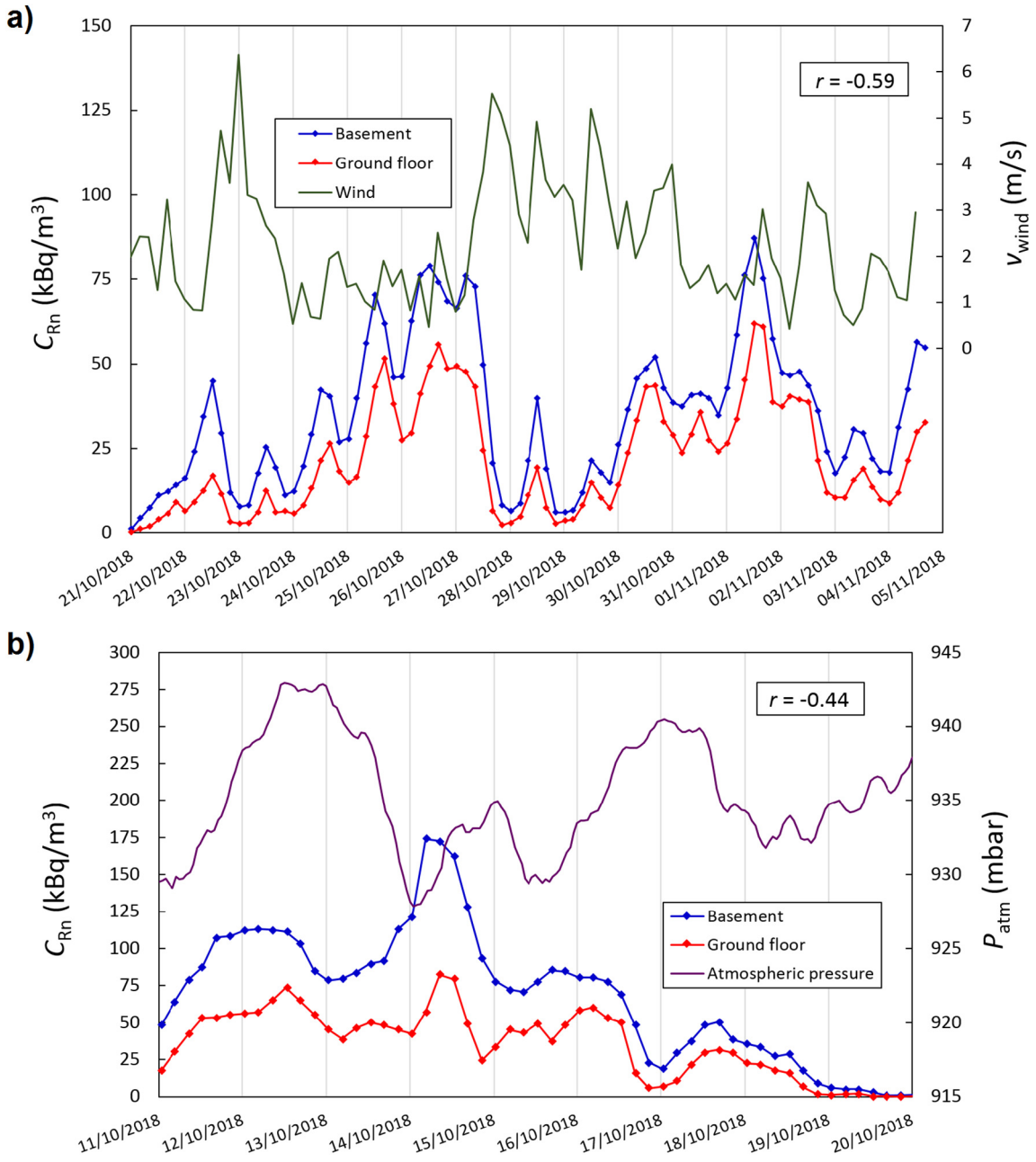

Fig. 6. Radon concentration recorded in the basement and ground floor of the pilot house along with atmospheric variables, a) wind velocity and b) atmospheric pressure, for different time periods while the house was closed. Pearson's correlation coefficient *r* between radon concentration in the basement and the corresponding atmospheric variable is indicated.

recorded, a negative correlation is found between the atmospheric pressure and radon levels, which is consistent with results from other investigations (Mentes and Eper-Papao, 2015). An example of such correlation between radon and atmospheric pressure is presented in Fig. 6(b), where radon concentration decreases with the increase of the atmospheric pressure with a time delay. Pearson's correlation coefficient found for this particular case is $r = -0.44$ with a 95% confidence level. No significant correlation with radon levels was found for the other two atmospheric parameters monitored in the study, relative humidity percentage and accumulated rain.

From the initial study conducted at the pilot house in 2006, the pressure difference created due to indoor-outdoor temperature differences is below 3 Pa, which is small compared to the pressure gradient created by other parameters such as the wind or atmospheric pressure. However, both temperature and wind are usually associated to atmospheric pressure changes, which is the key parameter affecting the radon levels in the pilot house, creating pressure differences in the order of magnitude of a few thousand Pa (Frutos, 2009).

This case study was focused on the impact of the soil depressurisation, so further investigation extended in time would be required to understand the radon behaviour in detail at the pilot house, as a function of all the atmospheric parameters and their time variations.

4. Soil depressurisation effectiveness analysis

The distribution of the pressure induced under the slab as a consequence of the soil depressurisation system performance, correlation between the extraction airflow and the depressurisation, and radon reduction are analysed below.

4.1. Pressure field extension

The pressure distribution under the pilot house was studied for different depressurisation induced at the central sump of the SD system, both by active and passive performance of the system. Prior to the depressurisation analysis, it was found that the pressure difference between the indoor air and the measurement points under the slab fluctuates around 0 Pa for the closed testing periods when there is no SD in operation. During the passive SD testing period, the pressure induced under the slab as a consequence of the wind force reached levels of approximately −20 Pa, for wind velocities up to 8 m/s. For the active SD operation, the pressure induced at the sump was up to −250 Pa for the highest power of the mechanical fan.

The analysis of the pressure data recorded under the slab for the different testing phases at distances $d = 1, 2$ and 2.4 m from the suction point, using the centre of the sump as the reference, leads to obtain the rate of pressure drop with distance across the slab, which is also related to the depressurisation generated (see Fig. 7).

Fig. 7 shows that the pressure drop with distance results are consistent for the measurements recorded at the different distances $d = 1, 2$ and 2.4 m from the suction point. The trend of the pressure drop with distance is linear with the depressurisation under the slab; therefore the lower the pressure induced under the slab, the higher the pressure drop with the distance. However, a quite homogenous PFE, not exceeding 1 Pa/m pressure drop rate was found with distance for the highest depressurisation tested, induced by the highest extraction airflow rate permitted by the fan during the active SD operation.

4.2. Depressurisation induced as function of the extraction airflow

Some results of the pressure induced under the slab as a function of the extraction velocity during the active SD performance are presented in Fig. 8. As mentioned above, the active SD testing depressurisation was generated by means of a mechanical fan and the extraction velocity was measured in the exhaust pipe directly under the extractor fan.

The highest depressurisation recorded under the slab during the active SD operation is approximately −250 Pa, induced by the highest extraction airflow rate of the mechanical fan equivalent to 4 m/s.

Abdelouhab et al. (2010) conducted a study of this kind in France at the MARIA (Mechanized house for Advanced Research on Indoor Air) experimental house, built with a 40 cm thick aggregate layer beneath the slab and two sumps, one centred and another decentred placed on the aggregate layer. They calculated two behaviour laws to relate the extraction airflow Q with the pressure difference induced between the aggregate layer and the inhabited volume ΔP for the natural and mechanical extraction. A similar behaviour law is obtained from the active SD experimental data of the monitoring study at the pilot house, the extraction airflow in this case is obtained from the mechanical fan velocity based on the exhaust pipe diameter (see Fig. 9).

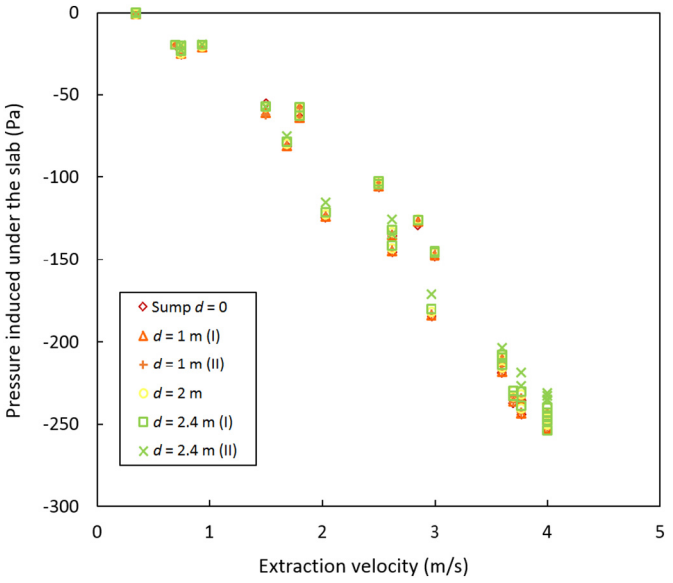

Fig. 8. Pressure induced under the slab during active SD operation against the extraction velocity of the mechanical fan for the different measurement points at different distances from the suction point.

The trendline fitting the experimental data for the active SD performance represents the permeability characterisation of the pilot house comprising the aggregate layer, ground and concrete slab, and is described by the following power law:

$$Q = (2.1 \pm 0.2)\Delta P^{(0.79 \pm 0.02)} \quad (2)$$

Experimental data obtained for the active SD performance in the pilot house are similar to the results for the active depressurisation in Abdelouhab et al. (2010). From Fig. 9 it is observed that the behaviour

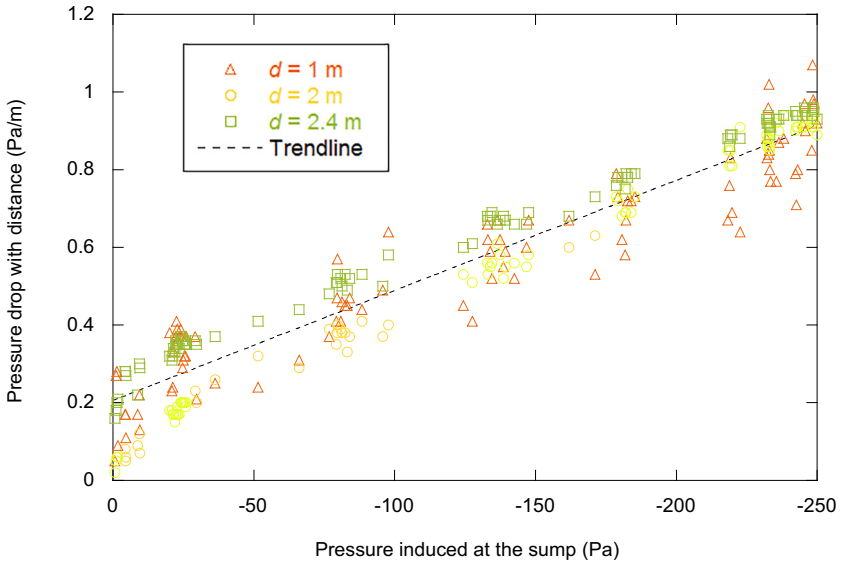

Fig. 7. Pressure drop with distance against pressure induced at the sump. Symbols represent the experimental data obtained from pressure records at distances $d = 1, 2$ and 2.4 m from the sump, both for active and passive SD testing phases. The dashed line is the linear trend obtained from all the experimental data, with a coefficient of determination $R^2 = 0.95$.

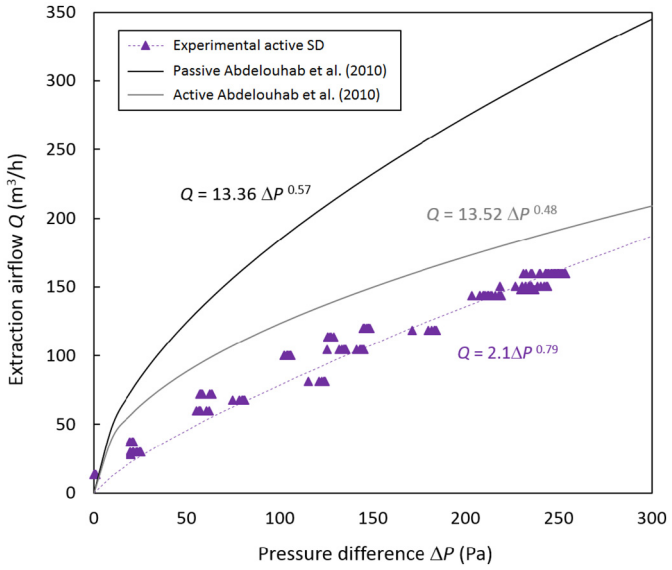

Fig. 9. Extraction airflow through the central exhaust pipe as function of the pressure difference generated between the aggregate layer under the slab and the inhabited volume of the basement. Symbols represent the experimental data for the active SD, the dashed line is the trend obtained from the experimental data and the solid lines represent the law relating extraction airflow with depressurisation for active and passive SD from Abdelouhab et al. (2010).

law differs for the active and passive SD operation in Abdelouhab et al. (2010), these results are explained by the fact that the permeability of the slab was modified due to works on it between tests. For the passive extraction the slab was leakier and higher extraction flow from the ground was induced to obtain the same depressurisation below the slab.

For a given airflow extraction rate from the ground, the depressurisation generated under the slab in the pilot house is the same no matter the phenomenon generating the extraction from the ground (active or passive), as it is determined by the permeability of the domain (aggregate layer, ground and slab). By solving Eq. (2), the theoretical extraction airflow required in the exhaust pipe of the pilot house to obtain a certain depressurisation under the slab can be calculated.

An example of the depressurisation generated under the slab by means of a rotating cowl during the passive SD operation is shown in Fig. 10(a) along with the wind velocity. There are no measurements of the extraction airflow generated in the exhaust pipe during the passive SD testing as a result of the wind effect. There are only records of the wind velocity, measured at the rooftop of the pilot house at a similar height to the rotating cowl and at a distance of approximately 3.5 m from the centre of the exhaust pipe. Fig. 10(b) shows the pressure induced at the sump as function of the wind velocity.

From data in Fig. 10(b) and using Eq. (2), a linear relationship between the wind velocity and the theoretical extraction airflow required in the exhaust pipe to induce such pressure under the slab is obtained (see Fig. 11). This relationship is only applicable to the type of rotating chimney cowl used during passive SD testing.

Following the results shown in Fig. 11, further passive SD testing phases would be required to investigate different type of extractors and chimney cowls in order to evaluate their performance at the pilot house, with known permeability from Eq. (2), and in line with research on the topic by Allard et al. (2018) and Hung et al. (2019).

4.3. Radon reduction

The radon reductions obtained for the different testing phases are summarised in Table 2, relative to the average radon concentration in the basement and ground floor calculated from the closed testing phases. It should be emphasised that the outdoor radon concentration in the area surrounding the pilot house is very high, approximately 300 Bq/m^3, while the average outdoor radon concentration globally is between 5 and 15 Bq/m^3 (WHO, 2016).

In all cases the radon reductions obtained are over 85%, and the highest reduction is found for the testing phase 4 reaching a radon concentration in the ground floor of 328 Bq/m^3, which is comparable to the outdoor radon concentration at the site, and a radon concentration of 662 Bq/m^3 in the basement. During phase 4 the mechanical fan was tested varying the extraction airflow and up to the highest power permitted (80 W).

From phase 6 experimental results, it can be highlighted that a 30 W mechanical fan, which is the equivalent power for the extraction airflow used during testing phase 6, is sufficient to reach radon reductions up to 94% in the basement and 86% in the ground floor in a house of these permeability characteristics. In terms of pressure induced under the slab, the average value at the sump recorded for testing phase 6 is −55 Pa.

Although it depends on the atmospheric conditions (mainly wind and temperature) and the occupant behaviour, the typical pressure difference found between indoors and the soil in a dwelling oscillates

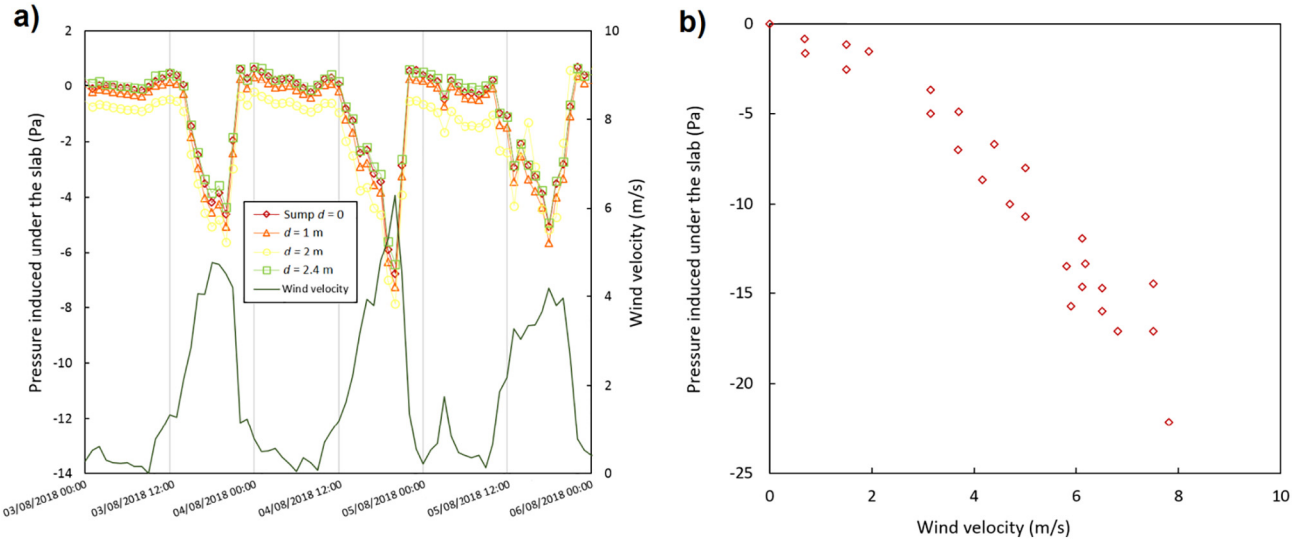

Fig. 10. (a) Hourly averaged pressure induced under the slab at the sump and the different measurement points with distances indicated from the central pipe along with hourly averaged wind velocity recorded at the site. (b) Pressure induced at the sump during passive SD operation against the wind velocity.

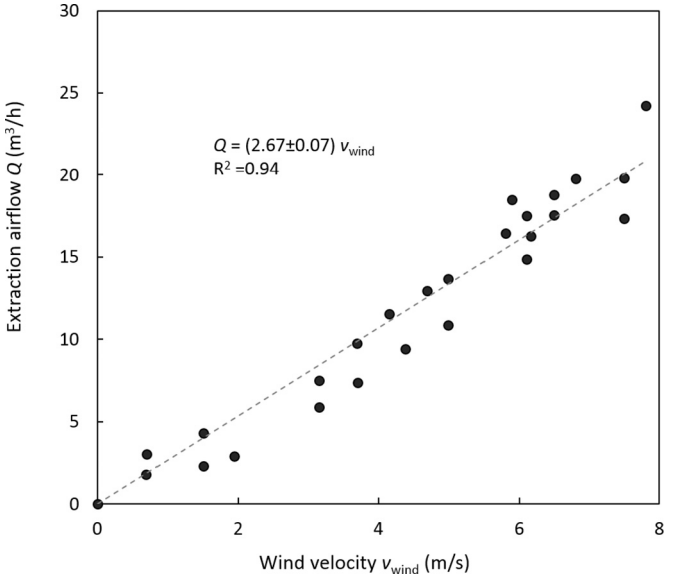

Fig. 11. Extraction airflow expected in the central exhaust pipe of the pilot house SD system against wind velocity, from measurements during passive SD testing by means of a rotating cowl. Dots represent the experimental data and the dashed line is the trendline obtained from the experimental data.

between 1 and 5 Pa. Thus, the depressurisation system should be designed to induce at least −6 Pa in every point of the slab area (Fowler et al., 1991; Broadhead, 2018; Dumais, 2018). Looking at Fig. 8, it can be observed that such pressure is obtained for extraction velocities below 1 m/s that correspond to 20 W power of the mechanical fan. Therefore, it could be postulated that a 20 W mechanical fan is sufficient to achieve an optimum soil depressurisation reaching radon reductions above 85% for dwellings with similar permeability characteristics to the experimental house studied here.

5. Conclusions

A monitoring study was conducted in a pilot house with extremely high radon levels to investigate the ability and efficiency of radon mitigation by both active and passive soil depressurisation. The study was motivated by the need to quantify SD effectiveness in terms of pressure field extension and also quantify significant radon reductions.

The testing plan consisted of different testing phases, alternating closed periods of the house to foster radon accumulation in the experimental house with SD operation phases. The variables monitored over the different testing periods were radon concentration in the basement and ground floor of the house, pressure field extension under the slab, and atmospheric parameters such as wind velocity, indoor and outdoor temperature, atmospheric pressure, relative humidity and accumulated rain.

Table 2
Radon concentration C_{Rn} found in the basement and ground floor for the SD testing phases indicated and radon reduction, respect to the average radon levels for the closed periods.

	C_{Rn} (Bq/m^3)		Radon reduction	
	Basement	Ground floor	Basement	Ground floor
Average closed	54,625	26,421		
Phase 2: passive SD	7417	–	86%	–
Phase 4: active SD (v_{ext} = 0–4 m/s)	662	328	99%	99%
Phase 6: active SD (v_{ext} = 1.5 m/s)	3326	3689	94%	86%
Phase 8: active SD (v_{ext} = 2 m/s)	3701	2279	93%	91%

Radon concentration behaviour was analysed for the closed testing periods, where an average radon concentration of 55 kBq/m^3 was found in the basement, while for the ground floor there was an average radon concentration of 26 kBq/m^3. Atmospheric variables influence on the radon behaviour in the house was also studied, finding significant correlations between outdoor temperature, atmospheric pressure and wind velocity with the radon concentration in the house. Impact of the indoor-outdoor temperature difference was discussed as well, significant negative correlation between pressure difference created as result of the temperature gradient with the radon concentration in the ground floor was obtained.

From the analysis of the pressure distribution under the slab, it was proven that the pressure drop with distance from the suction point of the SD system is linear with the depressurisation generated under the slab. Still, it was found that the distribution of the pressure under the slab in the pilot house is quite homogeneous, not exceeding 1 Pa/m pressure drop with distance for the highest depressurisation generated under the slab by active SD.

Permeability characterisation of the pilot house (including the aggregate layer, ground and concrete slab) was conducted, finding a behaviour law from the experimental data for the active SD performance, similar to previous works published on the characterisation of granular fill materials for radon soil depressurisation systems across Europe. Also, a relationship between the wind velocity and the extraction airflow from the ground was found for the passive SD performance by means of the particular rotating cowl used.

Finally, radon reductions in excess of 85% were achieved for the different testing phases in all cases. Based on the radon reduction results associated with the depressurisation generated under the slab as function of the extraction airflow for the active SD conditions considered, it was found that 20 W power for a mechanical fan is sufficient to achieve an optimum soil depressurisation reaching radon reductions above 85%.

To summarise, the case study presented contributes to the specification for optimum soil depressurisation systems performance and the findings encountered have applicability within similar building type dwellings with comparable aggregate layer permeability characteristics within the European context.

Authors' contributions

Mark Foley, Jamie Goggins, Carlos Sainz and Marta Fuente contributed to the initial research plan and the conception of the monitoring study. Marta Fuente, Carlos Sainz, Ismael Fuente and Daniel Rábago also evaluated and reviewed the testing plan. The experimental development of the study was conducted by Marta Fuente and Daniel Rábago with the help from the radon group technical staff (Enrique Fernández, Jorge Quindós and Luis Quindós) and the support of ENUSA Industrias Avanzadas S.A. Marta Fuente processed the experimental data, analysed the results with the help from Daniel Rábago and wrote the manuscript. Mark Foley, Jamie Goggins, Ismael Fuente and Carlos Sainz reviewed and edited the manuscript for the final version. All authors read and approved the final manuscript.

Declaration of Competing Interest

The authors declare that they have no known competing financial interests or personal relationships that could have appeared to influence the work reported in this paper.

Acknowledgments

This research was supported by the OPTI-SDS project carried out at the National University of Ireland Galway in collaboration with University of Cantabria, Spain. The OPTI-SDS project is funded by the Irish Environmental Protection Agency (EPA) [project code 2015-HW-MS-5].

The work was performed at the ENUSA Industrias Avanzadas S.A. facilities in Spain, thanks to the collaboration with the radon group at University of Cantabria. The authors would like to acknowledge ENUSA Industrias Avanzadas S.A. for the support and help while conducting the experiment and the technical staff of the radon group for their work on the experimental development of the study.

References

Abdelouhab, M., Collignan, B., Allard, F., 2010. Experimental study on passive soil depressurisation system to prevent soil gaseous pollutants into building. Build. Environ. 45, 2400–2406. https://doi.org/10.1016/j.buildenv.2010.05.001.

Allard, F., Abadie, M., Romani, Z., Burlot, M., Collignan, C., Druette, L., Peigné, P., Nicolle, J., 2018. Evaliation de la Performance des Systemes de Dépressurisation du Sol a Fonctionnement Natural (106 pages).

Baskaran, M., 2016. Radon: A Tracer for Geological, Geophysical and Geochemical Studies. Springer International Publishing https://doi.org/10.1007/978-3-319-21329-3 January.

Broadhead, B., 2018. Radon Mitigation in the US. WPB-Radon Inc. at ROOMS (Radon Outcomes on Mitigation Solutions) Conference (27th–28th September 2018, Lugano, Switerland). SUPSI.

Burke, O., Long, S., Murphy, P., Organo, C., Fenton, D., Colgan, P.A., 2010. Estimation of seasonal correction factors through Fourier decomposition analysis – a new model for indoor radon levels in Irish homes. J. Radiol. Prot. 30, 433–443. https://doi.org/10.1088/0952-4746/30/3/002.

Darby, S., Hill, D., Auvinen, A., Barros-Dios, J.M., Baysson, H., Bochicchio, F., ... Doll, R., 2004. Radon in homes and risk of lung cancer: collaborative analysis of individual data from 13 European case-control studies. BMJ 330 (7485), 223. https://doi.org/10.1136/bmj.38308.477650.63.

DELG, 2002. Radon in Existing Buildings. Corrective Options. Technical Report. Department of the Environment and Local Government, Stationery Office, Dublin.

Diallo, T.M.O., Collignan, B., Allard, F., 2015. Air flow models for sub-slab depressurization systems design. Build. Environ. 87, 327–341. https://doi.org/10.1016/j.buildenv.2015.01.017.

Dumais, C., 2018. The Canadian approach to radon mitigation and design. Radonwest Inc. at ROOMS (Radon Outcomes on Mitigation Solutions) Conference (27th–28th September 2018, Lugano, Switzerland). SUPSI.

Fowler, C.S., Williamson, A.D., Pyle, B.E., Belzer, F.E., Coker, R.N., 1991. Handbook: Sub-slab Depressurization for Low-permeability Fill Material. Design & Installation of a Home Radon Reduction System. US EPA, Washington, DC, USA.

Frutos, B., 2009. Estudio experimental sobre la efectividad y la viabilidad de distintas soluciones constructivas para reducir la concentración de gas radón en edificaciones. Universidad Politécnica de Madrid, Madrid.

Frutos, B., Olaya, M., Santiago, L., Poncela, Q., Sainz, C., 2011. Experimental study of effectiveness of four radon mitigation solutions, based on underground depressurization, tested in prototype housing built in a high radon area in Spain. J. Environ. Radioact. 102 (4), 378–385. https://doi.org/10.1016/j.jenvrad.2011.02.006.

Fuente, M., Rabago, D., Herrera, S., Quindos, L., Fuente, I., Foley, M., Sainz, C., 2018. Performance of radon monitors in a purpose-built radon chamber. J. Radiol. Prot. 38, 1111–1127. https://doi.org/10.1088/1361-6498/aad969.

Fuente, M., Muñoz, E., Sicilia, I., Goggins, J., Hung, L.C., Frutos, B., Foley, M., 2019. Investigation of gas flow through soils and granular fill materials for the optimisation of radon soil depressurisation system. J. Environ. Radioact. 198, 200–209. https://doi.org/10.1016/j.jenvrad.2018.12.024.

Garcia-Tobar, J., 2019. Weather-dependent modelling of the indoor radon concentration in two dwellings using CONTAM. Indoor Built Environ. 0 (0), 1–9. https://doi.org/10.1177/1420326X19841119.

Hung, L.C., Goggins, J., Fuente, M., Foley, M., 2018a. Characterisation of specified granular fill material for radon mitigation by soil depressurisation systems. Constr. Build. Mater. 176, 213–227. https://doi.org/10.1016/j.conbuildmat.2018.04.210.

Hung, L.C., Goggins, J., Fuente, M., Foley, M., 2018b. Investigation of sub-slab pressure field extension in specified granular fill materials incorporating a sump-based soil depressurisation system for radon mitigation. Sci. Total Environ. 637–638, 1081–1097. https://doi.org/10.1016/j.scitotenv.2018.04.401.

Hung, L.C., Goggins, J., Croxford, C., Foley, M., 2019. Large-scale experimental investigation of specified granular fill materials for radon mitigation by active and passive soil depressurisation. J. Environ. Radioact. 207, 27–36. https://doi.org/10.1016/j.jenvrad.2019.05.018.

IGME (Instituto Geológico y Minero de España), 2015. http://info.igme.es/ielig/LIGInfo.aspx?codigo=CI079, Accessed date: 1 July 2019 (Updated 30 June).

Jiranek, M., 2014. Sub-slab depressurisation systems used in the Czech Republic and verification of their efficiency. Radiat. Prot. Dosim. 162 (1–2), 64–67. https://doi.org/10.1093/rpd/ncu219.

Long, S., Fenton, D., Cremin, M., Morgan, A., 2013. The effectiveness of radon preventive and remedial measures in Irish homes. J. Radiol. Prot. 33, 141–149. https://doi.org/10.1088/0952-4746/33/1/141.

Mentes, G., Eper-Papao, I., 2015. Investigation of temperature and barometric pressure variation effects on radon concentration in the Sopronbanfalva geodynamic observatory, Hungay. J. Environ. Radioact. 149, 64–72. https://doi.org/10.1016/j.jenvrad.2015.07.015.

Nero, A.V., Gadgil, A.J., Nazaroff, W.W., Revzan, K.L., 1990. Indoor Radon and its Decay Products: Concentrations, Causes and Control Strategies. Technical report. Lawrence Berkeley Laboratory. University of California, Berkeley, CA, USA.

Riley, W.J., Gadgil, A.J., Bonnefous, Y.C., Nazaroff, W., 1996. The effect of steady winds on radon-222 entry from soil into houses. Atmos. Environ. 30, 1167–1176. https://doi.org/10.1016/1352-2310(95)00248-0.

Schubert, M., Mussolff, A., Weiss, H., 2018. Influences of meteorological parameters on indoor radon concentrations (^{222}Rn) excluding the effects of forced ventilation and radon exhalation from soil and building materials. J. Environ. Radioact. 198, 81–85.

Scivyer, C.R., Jaggs, M.P.R., 1998. A BRE Guide to Radon Remedial Measures in Existing Dwellings. Dwellings With Cellars and Basements. BRE.

WHO, 2016. https://www.who.int/news-room/fact-sheets/detail/radon-and-health, Accessed date: 4 May 2019 (Updated 30 June).

World Health Organization, 2009. Handbook on Indoor Radon. A Public Health Perspective. WHO Press, Geneva, Switzerland.

World Health Organization, 2018. WHO Housing and Health Guidelines.